Nat Hazards (2014) 70:395–414
DOI 10.1007/s11069-013-0818-4

ORIGINAL PAPER

Coastal vulnerability to sea-level rise: a spatial–temporal assessment framework

Oz Sahin · Sherif Mohamed

Received: 10 September 2012 / Revised: 27 May 2013 / Accepted: 28 July 2013 /
Published online: 3 August 2013

Abstract The scientific community is confident that warming of the Earth's climate is unequivocal. Sea-level rise, which poses potential threats to coastal areas, is one of the most recognised possible impacts of this climate change. The nonlinearities, complexities, and spatial and temporal lags are common characteristics of coastal processes driven by human and natural interaction. With the acknowledgement of the complexity and dynamic nature of coastal systems, this paper introduces a spatial–temporal assessment framework, for addressing both the temporal and spatial variations, when assessing the vulnerability of natural and human systems in coastal areas. The framework is based upon a combination of system dynamics (SD) modelling and geographical information systems by taking into account spatial (x, y, z) and temporal (t) dimensions. The strategy of the adopted approach is to use the loose coupling approach by which a spatial model component is incorporated into a SD model component through a data converter.

Keywords Dynamic spatial modelling · GIS · Inundation · Sea-level rise · Storm surge · Vulnerability assessment

1 Introduction

There is general consensus among scientists that the climate is significantly and inevitably changing. Warming of the climate system is now unequivocal (Solomon et al. 2007). As the Earth continues to warm, coastal communities across the world will increasingly be faced with rising sea levels, as well as changes in storm surge (SS) frequency and

O. Sahin (✉) · S. Mohamed
Griffith School of Engineering, Centre for Infrastructure Engineering and Management, Griffith University, Gold Coast, QLD 4222, Australia
e-mail: o.sahin@griffith.edu.au

S. Mohamed
e-mail: s.mohamed@griffith.edu.au

magnitude. It is well known that sea-level rise (SLR) will have profound implications for many coastal populations and the systems on which they depend (Brooks et al. 2006). Significantly, most infrastructure, settlements, and facilities are located near the coast. Existing near-coastal populations, within 100 km of a shoreline and within 100 m current sea level, are estimated at 1.2 billion people, with an average density nearly three times higher than the global average density (Small and Nicholls 2003). While coastal communities have benefitted from many advantages of living and working in these areas, inevitably they also face the threat of natural disasters.

SLR, at the estimated rate, may not pose an immediate threat to coastal areas; however, a higher sea level will provide a higher base for storm surges to build upon. Thus, storm events occurring in conditions of higher mean sea levels will enable inundation and damaging waves to penetrate further inland, increasing flooding, erosion, and the subsequent impacts on built infrastructure and natural ecosystems (Pearce et al. 2007). As a result, SLR will exacerbate the vulnerability of coastal populations and ecosystems via permanent inundation of low-lying regions, inland extension of episodic flooding, increased beach erosion, and saline intrusion of aquifers (McLean et al. 2001). With concern for the consequences of SLR and associated SS, the pressing issues for decision-makers (DM) are the assessment of vulnerability and the evaluation of adaptation measures. However, due to uncertainty in climate change predictions, many vulnerability and adaptation assessments and most town planning activities, which are based on an assumption that the sea level will remain stable in the future, are in a state of flux. Added to the dilemma is the realisation that the impacts of SLR will, most likely, be spatially non-uniform across the world (Nicholls et al. 2007). It is therefore essential for DMs to consider the dynamic and spatial characteristics of these changes in assessing the impacts of SLR when making decisions about future infrastructure and community life.

With this in mind, this study focuses on developing a spatial–temporal model (STM) to assess the whole situation and its interacting components in space and time. This will be achieved by combining two modelling approaches, namely system dynamics (SD) and geographical information system (GIS), to create a STM.

1.1 Vulnerability assessment (VA)

Creating a readily understandable link between the theoretical concepts of flood vulnerability and the day-to-day decision-making processes is one of the most important goals of assessing coastal flood vulnerability, which then can be encapsulated in an easily accessible tool (Balica et al. 2012). The Intergovernmental Panel on Climate Change (IPCC) defines vulnerability as (Parry et al. 2007):

> The degree to which a system is susceptible to, and unable to cope with, adverse effects of climate change, including climate variability and extremes. Vulnerability is a function of the character, magnitude, and rate of climate change and variation to which a system is exposed, its sensitivity, and its adaptive capacity.

This definition incorporates three main variables: (1) exposure, (2) sensitivity, and (3) adaptive capacity. Thus, vulnerability is a function of the exposure, sensitivity, and adaptive capacity of a system. Based on the IPCC definition, many researchers (Rosenzweig and Tubiello 2006; Dongmei and Bin 2009; Yusuf and Francisco 2009; Eriyagama et al. 2010; Webersik et al. 2010) present vulnerability in the form of the following function:

$$V = f(E, S, \mathrm{AC}) \tag{1}$$

where V = vulnerability, E = exposure, S = sensitivity, and AC = adaptive capacity.

In Eq. (1), time is not explicitly taken into account. Hence, vulnerability assessments, based on the above definition, have assumed that vulnerability is a static process and, so, have been conducted with reference to a target year (e.g. 2100) and sea-level rise prediction (e.g. 1 m) (DCCEE 2009; Wu et al. 2009; Wang et al. 2010). However, vulnerability is a dynamic process and should be considered as a dynamic continuum. Further, as the three elements constituting vulnerability interact with, and change in time and space, so does the vulnerability. To include the dynamic and spatial aspects of vulnerability, by considering the time and space dependency, vulnerability can be expressed as:

$$V(t, s) = f\{(E(t, s), S(t, s), \mathrm{AC}(t, s)\} \tag{2}$$

where t represents temporal dimension and s three spatial dimensions (x, y, and z).

The function V (t, s) represents four dimensions in describing the vulnerability of a particular system, region, or group with respect to time and space. While exposure may depend upon geography, both sensitivity and adaptive capacity are closely linked to existing conditions, which refer to current conditions in a region. For example, the extent of exposure may depend on the size of the population, its proximity to the source of hazard source, an individual's or communities' preparedness to the hazardous events, and the extent of the hazardous events. As shown in Fig. 1, depending on the changes in the climatic and non-climatic drivers (e.g. population growth), a system's vulnerability will increase or decrease over a certain interval of a time (dt).

In other words, the greater the exposure or sensitivity, the greater is the vulnerability. However, adaptive capacity is inversely related to vulnerability. So, the greater the adaptive capacity, the lesser is the vulnerability. Therefore, reducing the vulnerability would involve reducing exposure and sensitivity through increasing adaptive capacity.

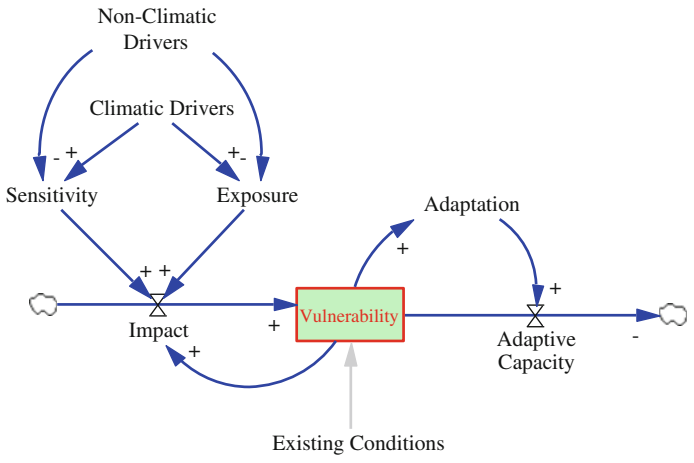

Fig. 1 Stock and flow representation of vulnerability varying over time, the *grey arrow* indicates conditions at the beginning of the simulation

2 Approach

The STM framework is based on space (x, y, z) and time (t), which constitute the four dimensions of the environmental dynamics and provide a common base where all natural and human processes occur. Using the STM, the coastal inundation is modelled to make predictions about what might happen with different actions under a number of SLR, population growth, and adaptation scenarios. A time-driven inundation model computes the condition (inundated or not inundated) in a cell on a square grid by advancing the simulation by fixed time intervals. Each cell in the grid contains an attribute value representing a characteristic of a corresponding location. For example, in a simulation for inundation, a cell can contain a value of 1 (*Sea*), 2 (*Waterway*), 3 (*Pond*), or 4 (*Land*) indicating the cell's state at each time step. The physical processes such as overland flow, and proximity to and connectivity of the area with neighbouring areas are important for modelling inundation caused by SS and SLR. At any time step, the condition of a cell can change if it satisfies certain criteria. To simulate this system, using the attribute values assigned for each cell, using the following logic, a cell at a location ($X_{i,j}$) will be flooded if the following two conditions are satisfied (Fig. 2):

1. The cell cover type CT ($X_{i,j}$) = L (not inundated), and the cover type of at least one of the adjacent cells CT ($X_{n,m}$) = W (a sea cell or inundated cell), and
2. The elevation of the cell CE ($X_{i,j}$) ≤the elevation of adjacent cell, CE ($X_{n,m}$).

The following function describes how the model predicts flood water diffusion from one cell to another:

$$F(X_{i,j}) = \begin{cases} 1, & \mathrm{CT}(X_{i,j}) = L \quad \text{and} \quad \exists x \mathrm{CT}(X_{n,m}) = W, \quad \text{and} \quad \mathrm{CE}(X_{i,j}) \leq \exists x \mathrm{CE}(X_{n,m}) \\ 0, & \text{otherwise} \end{cases} \tag{3}$$

where F is either flooded (1) or not flooded (0), CE represents the cell elevation, CT ($x_{i,j}$) represents the cover type, either inundated L or not inundated W, CT ($x_{n,m}$) represents the adjacent cells' cover types, either L land (or other cover types other than sea) or W sea (or became sea due to inundation), (n, m) refers to all adjacent cells to i, j (i.e. $i, j - 1$, $i, j + 1$, $i + 1, j$ and $i - 1, j$), and $\exists x$ is the existential quantification indicating that a logic is true for at least one member (x) of CT ($X_{n,m}$).

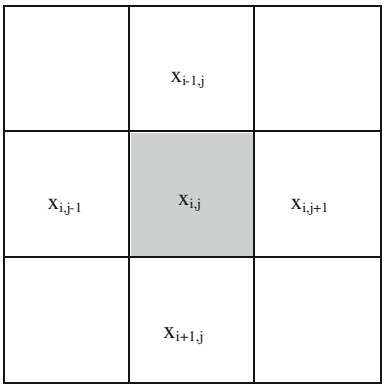

Fig. 2 Adjacent cells that determine the state of the cell ($X_{i,j}$). At any time step, the state can change if it satisfies certain criteria. The modelled space is portrayed as a three-dimensional grid (x, y, z)

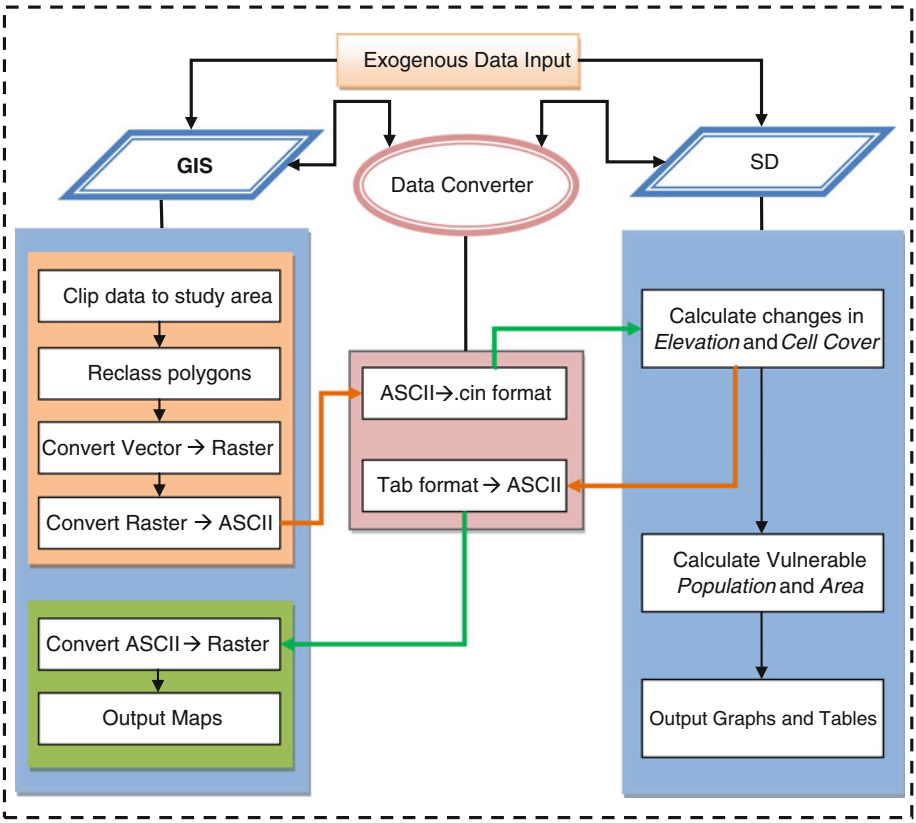

Fig. 3 Spatial–temporal model structure showing the process of vulnerability assessment using GIS, SD, and data convertor

The direction of the flooding, between the adjacent grid cells, depends on the difference in elevation between them. Using raster analysis through the cell connectivity and cell cover status testing, the model identifies potentially inundated areas based on elevation and proximity to the current shoreline or inundated areas (cells). Subsequently, using the above logic, the model labels all L raster cells adjacent to the neighbouring W cells and then performs a second order of analysis to identify cells whose elevation value is less than or equal to the W cells at each time step.

2.1 Spatial–temporal model (STM): coupling GIS and SD

An integral part of any vulnerability analysis is the aggregation methodology of its components (Holsten and Kropp 2012). The proposed STM consists of three components: GIS model, SD model, and the data monitor and converter, as shown in Fig. 3.

GIS and SD originated in and substantially different domains of expertise. Both have their own shortcomings. Although temporal process is adequately represented in SD models, spatial dimensions, however, are not explicitly dealt with. Conversely, GIS, while having strong capabilities of modelling the spatial dimensions of the real world, has difficulties in handling temporal dimensions. Combining the SD and GIS frameworks

provides the power in simultaneously addressing temporal and spatial problems as emphasised by several authors (Grossmann and Eberhardt 1992; Ruth and Pieper 1994; Ahmad and Simonovic 2004; Gharib 2008; Zhang 2008; Sahin and Mohamed 2013).

There are three common approaches for coupling GIS and SD: loose coupling, moderate integration and tight integration (Gimblett 2002; Maguire et al. 2005). There are trade-offs that are unique to each of the coupling strategies as each approach has its advantages and disadvantages. Although the loose coupling approach has some disadvantages, such as slow execution speed and low simultaneous execution capability, this approach is adopted to link SD and GIS in this study by considering some of its overpowering advantages (Maguire et al. 2005; Fedra 2006): ease of use, both GIS and SD can be modified and run in a straightforward manner; data structures do not have to be matched; data can be transformed to each other's formats through a converter; therefore, it does not require high-level programming expertise; users are able to make on-the-fly changes more rapidly; and it is fast and portable that the SD model can be used with different GIS.

2.2 Temporal model component

The temporal modelling consists of the building, integration and running of two types of models: an inundation model that addresses SLR and SS, and a vulnerability model that examines vulnerable population and areas. These submodels of the temporal components interact with each other through feedback links. The *Sea level* and *Population* variables are the two important drivers affecting inundation and vulnerability models. For the model, a hundred-year time horizon is considered; this scale is consistent with most SLR scenarios developed by the IPCC (Meehl et al. 2007).

When building the temporal model, the Vensim DSS® software is chosen. It is flexible when representing continuous or discrete time, a graphical interface, or performing causal tracing, optimisation, and sensitivity analysis (Ventana Systems 2012).

2.2.1 Inundation model

Figure 4 shows the inundation model structure and the key variables assumed to be important in a coastal system, and their interactions. As shown in Fig. 4, the system comprises three state variables: *Cell Cover*, *Elevation*, and *Sea Level*.

The *Sea Level* is an important variable causing change in both the *Elevation* and *Cell Cover* variables, over time. The model assumes a linear increase in the *Sea Level* over time, based on a range of SLR projections ranging from 0.5 to 1.5 m.

The SLR, at a given time, is calculated by:

$$\mathrm{SL}_t = \int \mathrm{d}R \times \mathrm{d}t + \mathrm{SL}_0 \tag{4}$$

where SL_t is the linear *Sea Level* at time t, dR is the rate of rise at each time step dt, and SL_0 is the initial *Sea Level* at the beginning of simulation.

For modelling purpose, the study area is subdivided into a cellular grid to simulate how floodwater spreads between adjacent cells, based on the conceptual framework for inundation. This grid is then superimposed over the coastal area. Each cell represents a specific area corresponding to one of four cover types: *Sea*, *Waterways*, *Pond*, and *Land*. At each simulation step, the state of each cell is determined by the condition of its neighbours to the north, east, south, and west. At each simulation step, as the sea level rises, the elevation

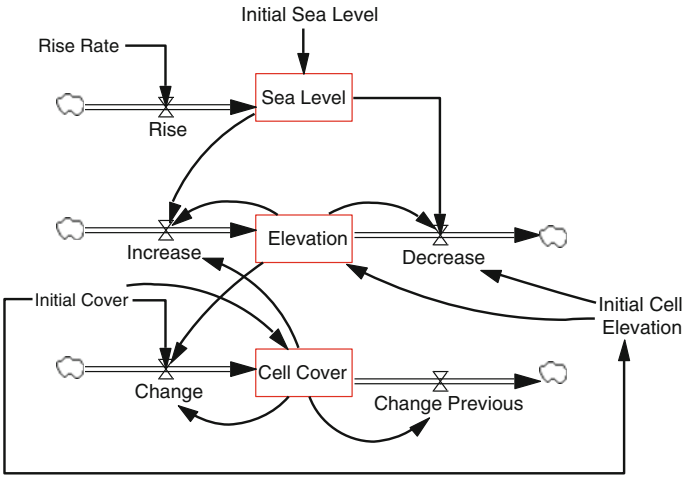

Fig. 4 Inundation model structure and key variables. The SLR scenarios, which drive other model components, can be altered to test the impact of varying rates of sea-level rise on the other model elements

of a cell is determined by its condition at the previous time step, its border conditions with its neighbours, and the cover type of its neighbours (*Land, Waterways, Sea,* and *Pond*). The elevation of a cell is determined by adjusting the elevation, at previous time steps, by the flow-in (*Increase*) and the flow-out (*Decrease*) of the cell, according to the properties of the adjacent cells. The *Elevation* is the integral of the net flow of *Increase* and *Decrease*, which is mathematically represented by the following equation:

$$E_t(x,y) = \int_0^t (I_t(x,y) - D_t(x,y)) \times \mathrm{d}t + E_0(x,y) \tag{5}$$

where E_t (x, y) represents cell elevation at location (x, y) at time t, E_0 (x, y) initial cell elevation at location (x, y) at time t_0, I_t (x, y) rate of elevation increase at location (x, y) at time t, and D_t (x, y) rate of elevation decrease at location (x, y) at time t

The changes in cell elevation occur when only the *Cover Type* of a cell is *Land*, *Waterways*, or *Pond*, at time step t_n, and it is transformed into *Sea* at the next time step, t_{n+1}. Here, the cell is assumed to be inundated from the rising sea level, and therefore, the elevation of the cell is updated and assumed to be equal to the *Sea Level* at the time period t_{n+1}. As the model commences, the state of the each cell at each time step is assessed simultaneously. The *Change* flows into the *Cell Cover* (Stock) and updates the *Cover Type* of the cell for the present time step (i.e. t_n). Subsequently, *Change Previous* removes the *Cell Cover* type of the cell at previous time step (i.e. t_{n-1}). This is necessary to assign only one cover type value to the cell for each time step. For example, if the *Change* alters the *Cell Cover* type of a cell from *Land* to *Water* at the time step t_1, then *Change Previous* discards the previous cover type value (*Land*) from the cell.

As explained in Sect. 3, the impacts of extreme changes in the sea level are analysed by determining how rising sea level would affect the average recurrence interval (ARI), as well as identify the height of current and future 1:100-year storm surges, over time. Then, the new ARI values are used by the vulnerability model to assess the impact of the storm events at each time step.

2.2.2 *Vulnerability model*

Vulnerability to SLR results from a combination of various factors, such as high population density along the coast and the susceptibility of coastal regions to coastal storms, as well as other effects of climate change. Therefore, an accelerated SLR could fundamentally change the state of the coast, and as a result, coastal environments and human populations will be affected significantly. In the final building step of the temporal model component, the vulnerability model is developed to estimate the potential impacts of SLR (Fig. 5). The critical vulnerability of coastal areas to coastal storms (in the short term) and SLR (in the long term) relates to flooding. Therefore, the vulnerability assessment (VA) needs to focus on people and properties. Hence, two VA indicators are selected:

1. *People at Risk* over time due to coastal flooding
2. *Area at Risk* (loss of land) due to inundation and coastal flooding

First, the number of people who live in the area is calculated based on two stocks in the model: the *Population* (P_0) that resides in the area at the beginning of simulation and the *Residents* (R_t), which is the integral factor of the *Population Increase* (P_t). The model determines the changes in population living in the area using the following equation:

$$R_t(x,y) = \int_0^t P_t(x,y) \times \mathrm{d}t + P_0(x,y) \tag{6}$$

where R_t (x, y) denotes people residing at location (x, y) at a given time, P_0 (x, y) initial number of people residing at location (x, y), and P_t (x, y) rate of population increase at location (x, y).

Then, *People at Risk* are calculated by multiplying the sum of *Flooded Area* with the *Cell Size*:

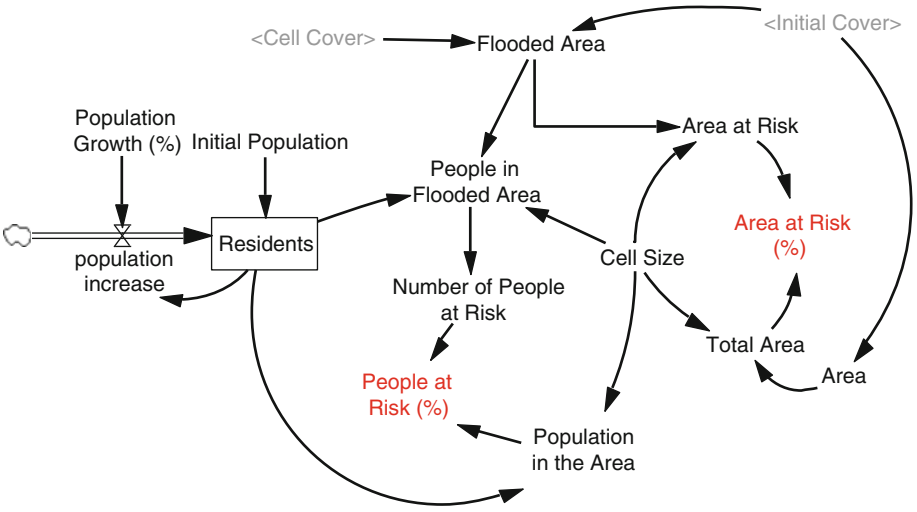

Fig. 5 Vulnerability model for estimating the potential impacts of SLR on people and property at risk

$$\mathrm{VP}_t = \sum R_t(x, y) \times \mathrm{FC}_t(x, y) \times Cs \tag{7}$$

where VP_t (x, y) represents vulnerable people at a given time, R_t (x, y) people residing at location (x, y) at a given time, Cs a constant value showing size of each grid cell, and FC_t (x, y) flooded area at location (x, y).

Then, the *Area at Risk* is calculated by multiplying the sum of the *Flooded Area* with the *Cell Size*:

$$A_t = \sum_{0}^{t} \mathrm{FC}_t(x, y) \times \mathrm{Cs} \tag{8}$$

where A_t (x, y) denotes vulnerable area at a given time, Cs a constant value showing size of each grid cell, and FC_t (x, y) flooded area at location (x, y).

2.3 Spatial model component

Spatial analysis is a set of methods whose results change when the locations of the objects being analysed change (Longley 2005). Importantly, spatial analysis derives information from the data using the spatial context of the problem and the data. That is, it deals with space. Geographical information system (GIS) is the main tool used in the spatial analysis. In this study, the ArcInfo 9.3.1 is used to develop the spatial model (ESRI 2009), which is connected to the temporal model through the data convertor and file monitor application developed for this framework by the authors.

There are two main ways to spatially model sea-level rise and subsequent coastal inundation using GIS. Geospatial data depict the real world in two forms, which leads to two distinct approaches: the *object-based* model and the *field-based* model (Goodchild 1992). The object-based method uses contour lines; it is usually suitable for a very rapid and simple risk assessment over large areas. However, it does not take into account the presence of intervening topographic ridges or other features (e.g. man-made defences) that can separate a low-lying area from the source of flooding (Brown 2006). That is, since a contour-line method relies solely on elevation data, inaccuracies arise when deriving a vulnerable zone based on this method because it does not consider connecting cells. The raster model, as Lo and Yeung (2007) define it, is one of the variants of the field-based models of geospatial data modelling. It is best employed to represent spatial phenomena that are continuous over a large area. For example, the raster data model uses a regular grid to cover the space; the value in each cell represents the characteristic of a spatial phenomenon at the cell location. In computing algorithms, a raster can be treated as a matrix with rows (y-coordinates) and columns (x-coordinates), and its values can be stored into a 2D array. These characteristics hence make integration of GIS and SD easier, especially since SD can easily use array variables for data manipulation, aggregation, and analysis. Therefore, the raster data model was selected for spatial modelling.

The basic elements of a raster model include the cell value, cell size, raster bands, and spatial reference (Chang 2006). Each cell in a raster has a value (integer or floating) representing the characteristic of a spatial phenomenon at the location denoted by its column and row (x, y). Depending on the data type, both integer and floating-point rasters are used in spatial modelling. For example, the research considers a sea-level rise of 0.5–1.5 cm/year. Thus, a floating-point raster is more suitable for the elevation data, as rise of sea level represents continuous numeric data with decimal digits, i.e. 10.125 m, 10.124,

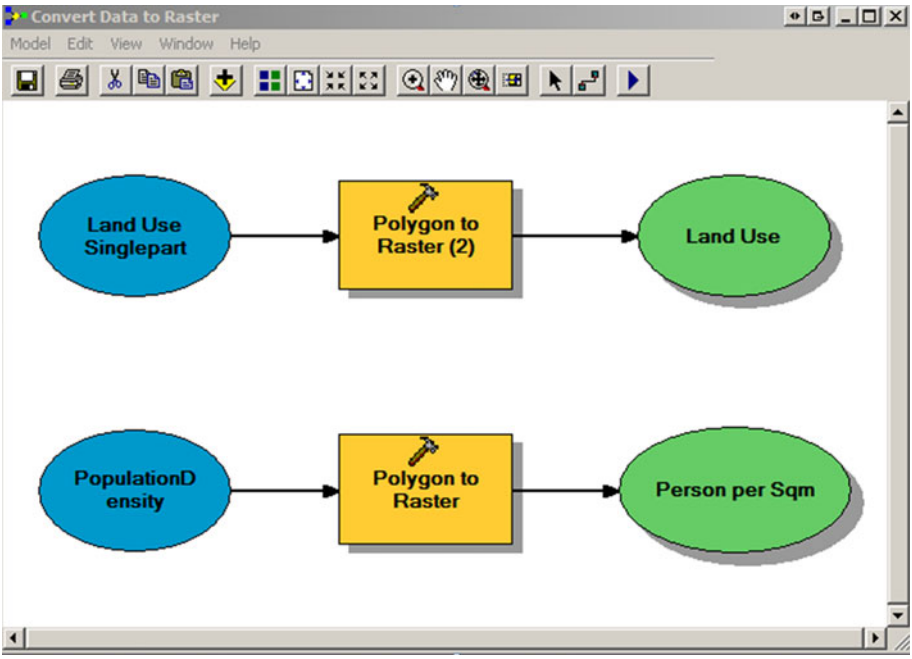

Fig. 6 Vector to raster conversion using the ArcGIS model builder

and so forth. However, the integer values are used for land cover rasters, i.e. 1 for *Sea*, 2 for *Waterways*, 3 for *Pond*, and 4 for *Land*.

Essentially, the cell size determines the resolution of the raster model. As a larger raster cannot provide the precise location of the spatial features, the model results may not be satisfactory. Nevertheless, the smaller cell size can address these problems, although their use increases the data volume and data processing time, considerably. There are always trade-offs between the quality of the model outcomes and the processing time. In this study, a 5 m cell size is used for the modelling. The elevation data are the most critical elements in assessing the potential impacts of rising sea level. The uncertainty of the elevation data affects the delineation of the coastal elevation zones. Most elevation data sets have vertical accuracies of several metres or even tens of metres (at the 95 % confidence level). Gesch (2009) argues that the mapping of submetre increments of sea-level rise is highly questionable, especially if the elevation data used have a vertical accuracy of a metre or more (at the 95 %). That is, the elevation uncertainty is much smaller for the more accurate elevation data. To keep the analysis reasonably manageable, this study has focused on the vertical accuracy. Therefore, to acquire more accurate results, the research used 5 m DEM with 0.1 m vertical accuracy.

A variety of data from different sources are required as inputs to the spatial model. All the data layers need to be in grid (raster) format, with a resolution of 5 $\times$ 5 m cell size. By working at a high spatial resolution, the model is able to reflect, accurately, the spatial changes in inundation resulting from the SLR. This approach provides a convenient way for describing the geoprocessing procedure in GIS. Hence, based on this approach, we begin by converting the shape files to the raster format, then reclassifying, and correcting their projection, and, finally, unifying the coordinate system by using the model builder (Fig. 6). The vector data are, consequently, converted to a raster format.

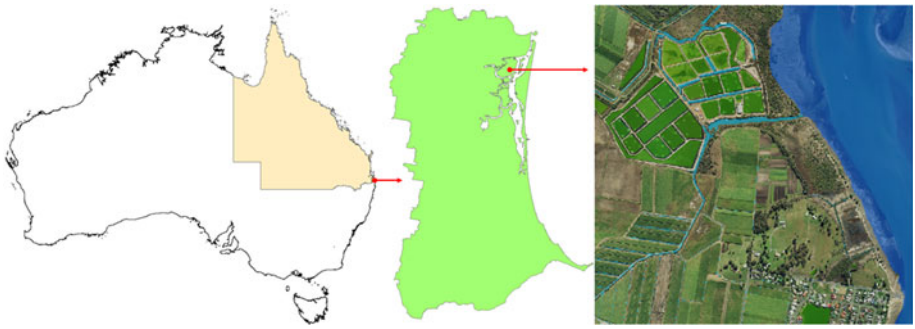

Fig. 7 Case study area: Gold Coast, south-east Queensland

The Model Builder is a graphical tool for automating a model through the use of a workflow. Spatially, the size of the raster cell generated was based on the minimum mapping unit (5 × 5 m) to match the DEM data. The attribute assignments are based on the centroid of the cell. Australian Bureau of Statistic (ABS) data on dwellings and the digital cadastral database (DCDB) are also converted to a raster format. Uncertainty, however, exists regarding where the population resides within the census parcel. Therefore, in the current study, the vulnerable population is estimated as a percentage of the census population, based on the inundated parcels.

2.4 Data converter

The loose coupling approach involves the transfer of data between the GIS and SD. Hence, it is necessary to establish, create, and manipulate data files, so that they can be exported or imported between the spatial and temporal components of the model. The data in the files can be stored in several file formats. Different file formats have different characteristics, depending on a range of factors, such as the source of the data, and the software architecture. As the STM combines two different modelling approaches, it is useful to choose a device-independent file format that can be usable by both applications, regardless of their hardware or software platforms. Therefore, in the current study, the device-independent ASCII file format for GIS, and the .cin and tab text file formats for SD are chosen for the cross-platform exchange of data. When exchanging data between two applications, it is necessary to convert the data formats into the right file format, as used by the applications (i.e. ASCII → .cin, and/or.cin → ASCII). To assist with this process, a converter program is developed.

The converter program involves two separate applications: the data converter and the file monitor. The data converter software automates the format transition between the ArcGIS and SD data formats. First, it converts the ArcGIS text (ASCII) files to SD text files (.cin), and then it converts the files from the SD.tab files back to the ArcGIS.txt files. All code for the data converter is written in C++ under Visual Studio 2008, using the Microsoft.NET framework version 2.0. As a console application, it takes its commands via program arguments (Fig. 7).

3 Implementing the STM approach

For case study analyses, north-eastern suburb of the Gold Coast City located in south-east Queensland, Australia, has been selected (Fig. 8). The area encompasses a diverse range of

features including sandy beaches, estuaries, coastal lagoons, and artificial waterways. In this region, the maximum tidal range is 1.8 m, and on average, the coast is affected by 1.5 cyclones each year (Boak et al. 2001). Many of the residential areas in the city are filled to the 1:100-year flood level (Betts 2002). Thus, the area is highly vulnerable to SLR.

To assess the impact of SLR in the case study area, especially in terms of land area being at risk of inundation, and the population being exposed to the consequences of this risk, the SLR was calculated for a given scenario and model, over a period of one hundred years. Based on these values in SLR, the STM was then used to estimate the area that would be inundated. Next, the possible impacts of SLR were estimated in terms of the population to be affected. The impact of storm events in the area was also assessed. Harper et al. (2000) projected that the highest projected storm tide levels (relative to the Australian Height Datum—AHD) within the region for 50, 100, 500, and 1,000-year storm events are 2.3, 2.5, 3.2, and 3.5 m, respectively. By using the trend line of these projections, Eqs. (9) and (10) were created and used to calculate the current conditions, the average recurrence interval (ARI), and the height of a given storm event:

Height:

$$y = 0.4094 \ln X + 0.6594 \tag{9}$$

ARI:

$$X = e^{((y-0.6594)/0.4094)} \tag{10}$$

To undertake this portion of the study, the height of a 1:100-year storm surge was added on top of the SLR estimation to project future SS levels. An apparent hypothesis was that some areas would become flood-prone, even if not permanently submerged. Further, the population and the properties within the area would also be affected by SLR and storm activities. Using these values, the STM was used to predict the extent of the flood-prone areas that would be affected by storm events. The results of the model, presented here, were generated using the SLR scenarios (ranging from 0.5 to 1.5 cm per year).

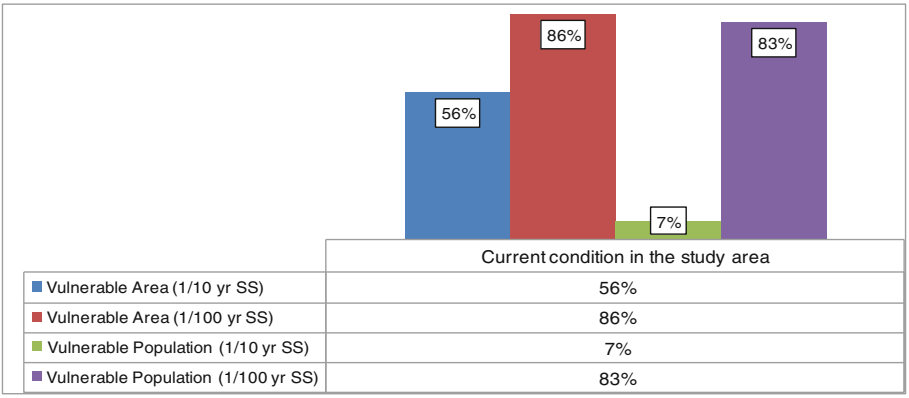

Fig. 8 Vulnerable area and population to current 1:10- and 1:100-year SS in the study area

4 Results and discussion

4.1 Current vulnerability assessment

To determine the populations and land areas at risk, the current vulnerability conditions were assessed. The 1:100-year flood levels (a measurement standard widely used for planning) were used to evaluate the area's vulnerability to coastal flooding. Based on the 1:100-year storm surge conditions (approximately a 2.5-m event), the vulnerable area and population were identified. The results indicate that the study area is already highly vulnerable to extreme conditions, such as 1:100-year storm events. Using the STM, with an assumption of zero SLR, currently 86 % of the land area and 83 % of the population are susceptible to 1:100-year storm events (Fig. 8). However, for a 1:10-year storm event (approximately a 1.6-m event), 56 % per cent of the land would be under threat of flooding, while only 7 % of the population would be affected. This analysis implies that a 0.9-m increase in storm surge height would cause a 76 % increase in the vulnerable population and an increase (though relatively smaller, at 30 %) in the vulnerable land area. Further, the assessment highlights that a 1:100-year storm event would have devastating impacts on the people residing in the inundated area.

4.2 Future vulnerability assessment

To determine the effect of changes in vulnerable populations and land areas over time, the *Cover Type* and *Elevation* data were simulated under a number of SLR and SS scenarios. The changes were captured in a SD model and exported to a GIS model for visualisation. The inundation layer was overlayed with the ABS census data, which was aggregated by census parcel for the area. The population was assumed to be distributed evenly within a parcel boundary. However, the STM allows the users to change the population projections so that they can better understand the impacts of the changing conditions. Within the future vulnerability assessments, the major land cover categories were as follows: *Sea*, *Waterways*, *Pond*, and *Land*. The storm surge heights were assumed to increase by the same amount as the SLR.

As seen from Table 1, as the magnitude of SLR increases, the area and the number of people vulnerable to flooding also rise. The results of the assessment indicate that at the end of a 100-year simulation period, approximately 6 % of the landscape in the study area will be inundated, with 0.5-cm SLR per year. Importantly, a 0.5-m SLR does not pose any significant threats to the local population. However, this situation dramatically changes with scenarios 2 and 3, which represent 1- and 1.5-cm SLR per year. Indeed, the percentage of the vulnerable area increased to about 34 % for scenario 2 and 56 % for scenario 3 (Table 1). Although a substantial fraction of the landscape is threatened by the rising SLR, the percentage of the population that can be classified as vulnerable is relatively low for scenario 2 and scenario 3, only 0.5 % and 7 %, respectively. The answer lies with most of the population residing at high altitudes. Nevertheless, the population located near waterways and coastal strips was especially vulnerable.

Further, as inundation occurs at the water–land interface, the land area in close proximity to the sea and around water bodies was identified as the most vulnerable area. The rising sea quickly penetrates inland through waterways and submerges the vulnerable areas around them, thus putting the people currently living in those areas at risk. Indeed, about 6 % of the study area landscape will be submerged if the sea level rises a 0.5 m by 2110 (Table 1). Hence, the area at significant risk will be increased, up to 34 and 56 % with a

Table 1 *Area at risk* and *Population at Risk* under three SLR scenarios

Scenarios	Years										
	2010	2020	2030	2040	2050	2060	2070	2080	2090	2100	2110
Area at Risk (%)											
0.5 cm/year	0	1.38	1.54	1.72	1.87	2.09	3.63	4.07	4.40	4.97	5.99
1 cm/year	0	1.48	1.87	3.63	4.40	5.95	9.39	13.75	19.24	26.90	33.89
1.5 cm/year	0	1.60	3.63	4.89	9.39	15.89	26.65	35.78	42.90	47.90	55.70
Population at Risk (%)											
0.5 cm/year	0	0	0	0	0	0	0.01	0.02	0.02	0.03	0.03
1 cm/year	0	0	0	0.01	0.02	0.03	0.07	0.13	0.18	0.33	0.48
1.5 cm/year	0	0	0.01	0.03	0.07	0.15	0.33	0.54	0.92	1.48	7.06

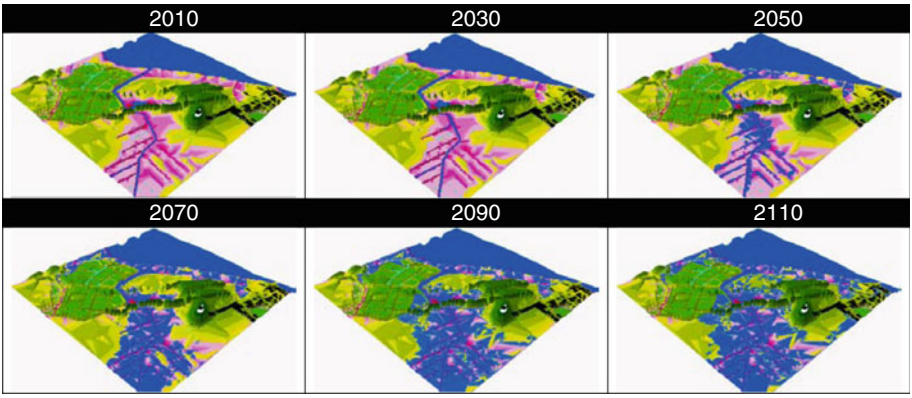

Fig. 9 Flood maps generated by the model using a 1.5 cm/year SLR scenario

1-m and 1.5-m rise in sea level, respectively. However, the inundation will, generally, be restricted to fringing shorelines and finger waterways margins. Figure 9 presents a series of flood maps generated by the model for a 1.5 cm/year scenario. It shows the extent of the areas at risk due to rising sea level, over a period of 100 years. Although up to 56 % of the land area will be facing the risk of inundation, the impacts of the same SLR scenarios on the residential areas are much smaller.

The simulation results predict that the residents in the area are safe from a SLR of up to 1 m. Nonetheless, about 7 % of residents face the risk of inundation with a 1.5-m rise in sea level within 100 years (Table 1). It appears that the year 2100 is a critical point; the analysis shows that the threat posed by a 1.5-m SLR demonstrates a sharp increase, jumping from about 1.5 to 7 %. Thus, a 1.5-m SLR may be the tipping point that leads to a rapid and irreversible change in the inundation area.

To compute the potential impacts of a rising sea level on already highly vulnerable populations and land areas, along with a 1:100-year storm event, the current 1:100-year SS height was gradually increased by 0.5, 1, and 1.5 cm per year, over a hundred-year period. This adjustment was based upon the SLR scenarios previously used. As shown in Table 2, a rising sea level will further increase the cumulative percentage of the vulnerable population and land area. As a result, and depending on the SLR scenario, vulnerabilities

from a 100-year SS will increase from 4 to 7 % for the population, and between 8 and 11 % for the land area. This outcome indicates only a small increase, as the area is already highly vulnerable to a current 100-year SS event. Nevertheless, this small increase, combined with the increase in ARI, would be devastating. Specifically, the impact will be more frequent and more damaging floods that increase the size of the coastal floodplain, placing new areas at risk for the first time.

4.3 Model refinement: assessment of adaptation options

The temporal model, introduced above, takes into account key variables that predict the extent and timing of coastal inundation. However, no variable was available to represent the adaptation alternatives. Thus, the model simulations were conducted under the *Take No Action* strategy. By modifying the model, 14 successive simulations were performed, with various values, to explore the impact of the *Build Protective Structure* and *Improve Building Design* adaptation options on vulnerable people and areas, as seen in Fig. 10.

First, to test the efficiencies of *Build Protective Structure*, the model was modified by adding a variable to represent an imaginary protective structure along the shoreline. The term "*Build Protective Structure*" refers to coastal engineering activities that reduce the risk of flooding and inundation. The heights of the protective structure varied from 0 to 2.5 m to estimate the most effective height that provided the best protection. The imaginary wall was built by altering the initial elevations of the border cells whose initial cover types were *Land* and adjacent to cells with *Sea.* Secondly, to test the efficiency of the *Improve Building Design* option, the model was further modified by adding another variable (*Improve Building Design*).

A comparison was made of the efficacy of building a 1 or 2 m high protective structure to reduce vulnerable areas to a 1.5-cm SLR per year. The findings show that building protective structures along the coastline does not have any effects on reducing the extent of the inundation under scenario 3 and, therefore, does not reduce the vulnerability. Similarly, *Protective Structures* (both 1 and 2 m) will not provide any safeguard for the vulnerable population from rising sea level. Secondly, to test the efficiency of the *Improve Building*

Table 2 Increase in *Area* and *Population at Risk* of 1:100-year SS due to SLR

Years	People at risk of 1:100-year SS (%)			Area at risk of 1:100-year SS (%)		
	SLR = 0.5 m (%)	SLR = 1 m (%)	SLR = 1.5 m (%)	SLR = 0.5 m (%)	SLR = 1 m (%)	SLR = 1.5 m (%)
2010	0	0	0	0	0	0
2020	1	2	3	2	3	4
2030	1	2	3	3	5	6
2040	2	3	3	4	6	7
2050	2	3	4	5	7	8
2060	2	4	5	6	8	9
2070	3	4	5	6	8	9
2080	3	5	5	7	9	9
2090	3	5	6	7	9	10
2100	3	5	6	7	9	10
2110	4	5	7	8	9	11

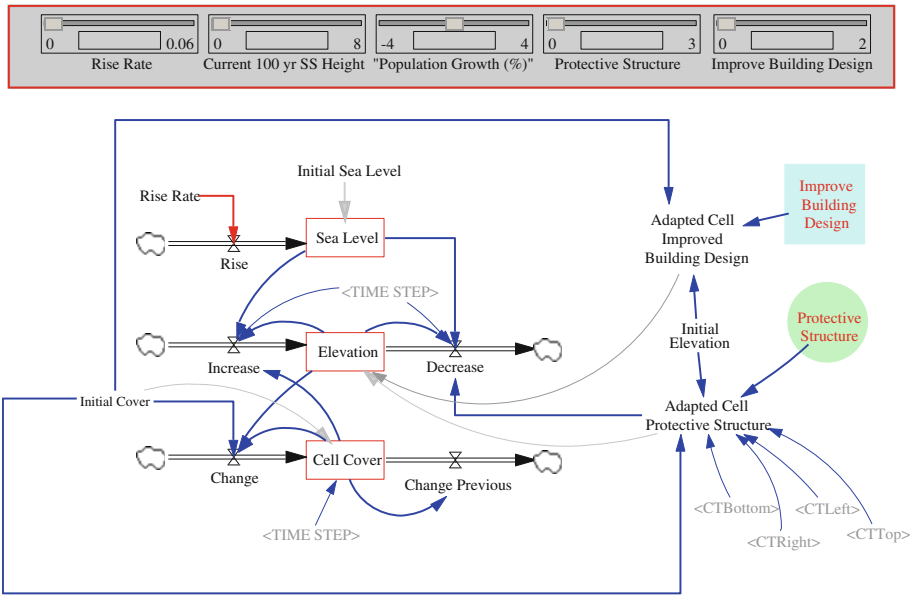

Fig. 10 Modified temporal model with *Improve Building Design* variable

Design option, the model was further modified by adding another variable (*Improve Building Design*). The *Improve Building Design* option covers a wide range of adaptation measures, including (but not limited to) flood proofing, elevated building design, and minimum flood level. As it was not possible to test each adaptation measure under this category, the focus was specifically on two measures: *elevated building design* and *minimum flood level*. Further, it was assumed that new building regulations would be introduced and that all existing and new buildings would be modified and/or designed accordingly. Based on these assumptions, the initial elevation of each cell with a *Land* cover type was increased by 1 m, and then 2 m.

The simulations were carried out by setting initial values for the three variables, then changing these values to test this adaption option under a range of SLR and SS scenarios. For this simulation, the values of the variables *Rise Rate* (min 0.005 m/y and max 0.015 m/y), *Current 100 year SS Height* (min 0 and max 2.5 m), and *Improve Building Design* (min 1 m and max 2 m) were altered within the range shown in brackets. The simulation results predicted that with a 1.5-m SLR over a 100-year period, 56 % of the land area would be submerged. However, implementing the option *Improved Building Design* reduced the vulnerability down to 6.5 and 0.1 % for a 1-m and 2-m building elevation, respectively. In contrast, the *Improved Building Design* adaptation option provided the vulnerable population with 100 % protection. The results demonstrate that elevating structures by the amount of the SLR, or more, would keep these structures at the same elevation relative to the sea and, thereby, prevent becoming more vulnerable as the sea level rises.

Using the simulation results, the impacts of the three adaptation options were compared. The outcomes on vulnerable people and areas are shown in Table 3. Firstly, the *Build Protective Structure* adaptation option was not an effective strategy in reducing vulnerability to SLR and associated SS. Secondly, the presence of rivers and canals in the study area nullified the effectiveness of any protective structures against SS and SLR, especially

Table 3 Impacts of three adaptation options in reducing vulnerability of population and area to SLR and SS

Adaptation option	1.5-m SLR		1.5-m SLR + storm surge	
	Area	Population	Area	Population
Take No Action	56.0	7.1	92.2	93.1
Protective Structure (1 m)	56.0	7.1	92.2	93.1
Improve Building Design (1 m)	6.5	0.0	89.3	90.4
Protective Structure (2 m)	55.4	7.1	92.2	93.1
Improve Building Design (2 m)	0.1	0.0	79.7	54.6

when combined with heavy rainfall and flash flooding. Thirdly, as the sea level rises, flooding penetrates into the same places it has occurred before. However, the *Improve Building Design* option offers a much better option against SS with a 1.5 cm/year SLR. As demonstrated above, this option has the potential to reduce, significantly, the vulnerabilities to a 1.5-m SLR. On the other hand, its shielding power diminishes against a 1.5-m SLR combined with SS.

5 Limitations and recommendations

All research has limitations, and this one is no exception. One of the limitations of the scope of this research is that it only addresses the impacts on communities and land area from inundation and coastal flooding. All other impacts, such as flooding due to heavy precipitation, are disregarded. Thus, future research could examine the other types of coastal impacts to determine their impacts on natural and socio-economic systems through examining the relationships between the impacts of rapid population growth, together with the gradual expansion of the urban area, and the frequency and magnitude of coastal inundations, using a more detailed socio-economic scenario linked to the STM.

Additionally, the economic and social costs related to SLR and SS were not addressed by the current research as these areas did not fit within the research scope. Future research could investigate the cost of adaptation, such as property values, loss of income, and cumulative effects of multiple options, and provide greater specificity to the potential adaptation perspectives and implementation measures of a number of the adaptation options, especially those associated with the building and infrastructure standards. Further development of cross-sectoral frameworks of policies and programmes should also form part of this future research.

6 Conclusions

Faced with increased threats from accelerated SLR and associated storm surge events, there is an urgent need for coastal communities to act faster to adapt to SLR, to reduce any potential destructive impacts, and to develop more effective policies. Developing effective policies requires more accurate information to strengthen the DMs' ability to make more effective decisions, with greater speed and accuracy. Determining how and when specific actions should be taken, however, is not a simple decision. Addressing the climate change problems and evaluation of potential adaptation responses should be informed by systematic analysis of potential impacts and the adaptive capacities of the system under

investigation. But, in order to generate the information needed to inform options for adaptation responses, these impact and adaptive capacity analyses must be assimilated through the intermediate step of a vulnerability assessment. Further, as vulnerability is location-specific and because a large share of decisions affecting vulnerability is made locally, the local-level VA is an important instrument for decision-making (Næss et al. 2006).

In this context, the STM approach, through generating valuable spatial–temporal information, lays the foundation for making decision on appropriate adaptation strategy. The technical focus centred on demonstrating one of the practical ways in which the functionalities of GIS and SD can be enhanced through their integration building a STM. The work provides insights into the complex coastal systems, while also evaluating efficiency of some adaptation options. Importantly, the approach enables DMs to critically examine the decision alternatives through the use of the SD component of the STM. Vital components in a successful decision-making process are the thoughtful communication of the uncertainties and the active participation of the stakeholders. Significantly, the research outcomes confirm that the utilisation of STM enables the DMs for actively addressing uncertainties and generating alternative scenarios based on different inputs to the models. Thus, the current approach facilitated both components. Further, the practical implications of the research encompass the development of a model to assist DMs to better understand coastal processes, identify vulnerabilities more accurately and effectively, evaluate some adaptation options, and improve decision-making about where to focus protection and adaptation efforts once vulnerabilities of the areas and the specific assets (people, hot spot places, buildings, critical infrastructure, and natural resources) are identified.

In this context, to support realistic decision-making, the VA results can be incorporated into asset management, emergency and risk management, flood mitigation management, communication of climate change, and stakeholder management. As a result, the STM would provide an important tool to support decisions made in relation to climate adaptation and the development of adaptation programmes.

In summary, the lack of scientific knowledge, the uncertainty associated with climate science and future risks from natural hazards, and the political sensitivities in dealing with climate change is seen as a barrier to effective adaptation. Understanding the implications of vulnerability assessment with respect to coastal settlements is a necessary undertaking to confirm the adequacy of current and future adaptation options, to improve our understanding of (extreme) adaptation, and to identify gaps in response and recovery to natural hazards in particular. However, the political sensitivities, technical difficulties, and the uncertainty of climate science make this a challenging undertaking. Nevertheless, these aims could be achieved, as demonstrated with this paper, through the use of STM providing information much needed for adapting the most vulnerable communities to changing climate.

Acknowledgments The authors gratefully acknowledge the funding from the Griffith Climate Change Response Program (GCCRP) and the Centre for Infrastructure Engineering and Management (CIEM)—Griffith School of Engineering.

References

Ahmad S, Simonovic SP (2004) Spatial system dynamics: new approach for simulation of water resources systems. J Comput Civil Eng ASCE 18:331–340

Balica S, Wright N, van der Meulen F (2012) A flood vulnerability index for coastal cities and its use in assessing climate change impacts. Nat Hazards 64:73–105
Betts H (2002) Flood damage analysis using GIS at Gold Coast Council. Aust J Emerg Manag 17:33–37
Boak L, McGrath J, Jackson LA (2001) A case study: the Northern Gold Coast beach protection strategy. In: Edge BL (ed) 27th international conference on coastal engineering, Sydney, Australia. American Society of Civil Engineers, pp 3710–3717
Brooks N, Hall J, Nicholls R (2006) Sea-level rise: coastal impacts and responses. The German Advisory Council on Global Change (WBGU), Berlin
Brown I (2006) Modelling future landscape change on coastal floodplains using a rule-based GIS. Environ Model Softw 21:1479–1490
Chang K-T (2006) Introduction to geographic information systems. McGraw-Hill Higher Education, Boston
DCCEE (2009) Climate change risks to Australia's coast: a first pass national assessment. The Department of Climate Change and Energy Efficiency, Canberra, Australia
Dongmei J, Bin L (2009) Countermeasures of adaptation to climate change: establishment and application for implementation matrix. Ecol Econ 5:102–111
Eriyagama N, Smakhtin V, Chandrapala L, Fernando K (2010) Impacts of climate change on water resources and agriculture in Sri Lanka: a review and preliminary vulnerability mapping. IWMI Research Report 135. Colombo, Sri Lanka: International Water Management Institute
ESRI (2009) ArcInfo. ESRI, Redlands, CA
Fedra K (2006) Beyond GIS: integrating dynamic simulation models and GIS for natural resources and environmental management. In: Conference proceedings of middle east 2006. Dubai, UAE
Gesch DB (2009) Analysis of lidar elevation data for improved identification and delineation of lands vulnerable to sea-level rise. J Coast Res 25(6):49–58
Gharib S (2008) Synthesizing system dynamics and geographic information systems in a new method to model and simulate environmental systems. PhD, University of Bergen
Gimblett HR (2002) Integrating geographic information systems and agent-based modeling techniques for simulating social and ecological processes. Oxford University Press, Oxford; NY
Goodchild MF (1992) Geographical data modeling. Comput Geosci 18:401–408
Grossmann WD, Eberhardt S (1992) Geographical information systems and dynamic modelling: potentials of a new approach. Ann Reg Sci 26:53–66
Harper B, Granger K, Jones T, Stehle J, Lacey R (2000) Tropical cyclone risks. In: Granger K, Hayne M (eds) Natural hazards and the risks they pose to South-East Queensland. Australian Geological Survey Organisation and Bureau of Meteorology, Canberra
Holsten A, Kropp JP (2012) An integrated and transferable climate change vulnerability assessment for regional application. Nat Hazards 64(3):1977–1999
Lo CP, Yeung AKW (2007) Concepts and techniques of geographic information systems. Pearson Prentice Hall, Upper Saddle River, NJ
Longley P (2005) Geographical information systems and science, 2nd edn. Wiley, Chichester
Maguire D, Batty M, Goodchild M (2005) GIS, spatial analysis, and modeling. Redlands, CA, USA, ESRI Pres
McLean RF, Tsyban A, Burkett V, Codignotto JO, Forbes DL, Mimura N, Beamish RJ, Ittekkot V (2001) Coastal zones and marine ecosystems. Climate Change 2001: Impacts, Adaptation, and Vulnerability Cambridge, UK and NY, USA
Meehl GA, Stocker TF, Collins WD, Friedlingstein P, Gaye AT, Gregory JM, Kitoh A, Knutti R, Murphy JM, Noda A, Raper SCB, Watterson IG, Weaver AJ, Zhao ZC (2007) Global climate projections. Climate change 2007: the physical science basis. Contribution of working group I to the fourth assessment report of the intergovernmental panel on climate change, The IPCC, Cambridge, UK and New York, NY, USA
Næss LO, Norland IT, Lafferty WM, Aall C (2006) Data and processes linking vulnerability assessment to adaptation decision-making on climate change in Norway. Glob Environ Change 16:221–233
Nicholls RJ, Wong PP, Burkett VR, Codignotto JO, Hay JE, McLean RF, Ragoonaden S, Woodroffe CD, Parry ML, Canziani OF, Palutikof JP, van der Linden PJ, Hanson CE (2007) Coastal systems and low-lying areas. Climate change 2007: impacts, adaptation and vulnerability. Contribution of working group II to the fourth assessment report of the intergovernmental panel on climate change. Cambridge, UK
Parry M, Canziani O, Palutikof J (2007) Technical summary. Climate change 2007: impacts, adaptation and vulnerability. In: Parry ML, Canzaiani OF, Palutikof JP, Van Der Linden PJ, Hanson CE (eds) Contribution of working group II to the fourth assessment report of the intergovernmental panel on climate change. Intergovernmental Panel on Climate Change, Cambridge, UK
Pearce K, Holper P, Hopkins M, Bouma W, Whetton P, Hennessy K, Power S (2007) Climate change in Australia Technical Report 2007, Canberra, Australia

Rosenzweig C, Tubiello FN (2006) Developing climate change impacts and adaptation metrics for agriculture. Global Forum on Sustainable Development on the Economic Benefits of Climate Change Policies, Paris

Ruth M, Pieper F (1994) Modeling spatial dynamics of sea-level rise in a coastal area. Syst Dyn Rev 10:375–389

Sahin O, Mohamed S (2013) A spatial temporal decision framework for adaptation to sea level rise. Environ Model Softw 46:129–141

Small C, Nicholls RJ (2003) A global analysis of human settlement in coastal zones. J Coastal Res 19:584–599

Solomon S, Qin D, Manning M, Chen Z, Marquis M, Averyt KB, Tignor M, Miller HL (2007) Summary for policymakers. Climate change 2007: the physical science basis. Contribution of working group I to the fourth assessment report of the intergovernmental panel on climate change

Ventana Systems (2012) Vensim DSS. 6.0b ed. Ventana Systems, Inc., Harvard, MA

Wang X, Smith MS, McAllister R, Leitch A, McFallan S, Meharg S (2010) Coastal inundation under climate change: a case study in South East Queensland. Climate adaptation flagship working paper No. 6. CSIRO

Webersik C, Esteban M, Shibayama T (2010) The economic impact of future increase in tropical cyclones in Japan. Nat Hazards 55:233–250

Wu S-Y, Najjar R, Siewert J (2009) Potential impacts of sea-level rise on the Mid and Upper-Atlantic Region of the United States. Clim Change 95:12–138

Yusuf AA, Francisco H (2009) Climate Change Vulnerability Mapping for Southeast Asia. Economy and Environment Program for Southeast Asia (EEPSEA), Singapore

Zhang B (2008) A study of GIS-SD based temporal-spatial modelling of water quality in water pollution accidents. In: ISPRS Congress Beijing 2008, proceedings of commission II. Beijing Reed Business, Geo